AD-A121 632 BEAM BREAKUP AND IMAGE DISPLACEMENT INSTABILITIES IN 1/1
HIGH CURRENT ELECTRO.. (U) MISSION RESEARCH CORP
ALBUQUERQUE NM B B GODFREY ET AL. SEP 82 AMRC-R-410
UNCLASSIFIED N00014-81-C-0647 F/G 20/7 NL

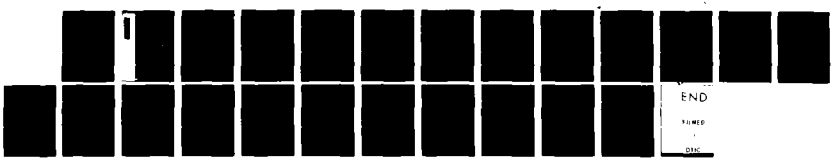

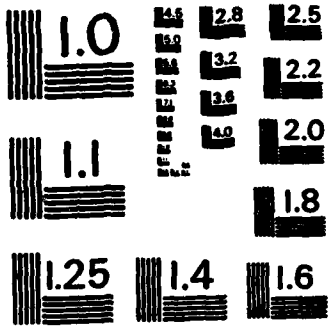

(12)

AMRC-R-410
Copy 25

BEAM BREAKUP AND IMAGE DISPLACEMENT INSTABILITIES IN HIGH CURRENT ELECTRON BEAM RACETRACK INDUCTION ACCELERATORS

B. B. Godfrey
T. P. Hughes

September 1982

Prepared for: Office of Naval Research
800 North Quincy Street
Arlington, Virginia 22207

Under Contract: N00014-81-C-0647

Prepared by: MISSION RESEARCH CORPORATION
1720 Randolph Road, S.E.
Albuquerque, New Mexico 87106

UNCLASSIFIED

SECURITY CLASSIFICATION OF THIS PAGE (When Data Entered)

REPORT DOCUMENTATION PAGE		READ INSTRUCTIONS BEFORE COMPLETING FORM
1. REPORT NUMBER	2. GOVT ACCESSION NO. AD-A121 632	3. RECIPIENT'S CATALOG NUMBER
4. TITLE (and Subtitle) BEAM BREAKUP AND IMAGE DISPLACEMENT INSTABILITIES IN HIGH CURRENT ELECTRON BEAM RACETRACK INDUCTION ACCELERATORS		5. TYPE OF REPORT & PERIOD COVERED INTERIM 6. PERFORMING ORG. REPORT NUMBER AMRC-R-410
7. AUTHOR(s) B. B. Godfrey and T. P. Hughes		8. CONTRACT OR GRANT NUMBER(s) N00014-81-C-0647
9. PERFORMING ORGANIZATION NAME AND ADDRESS MISSION RESEARCH CORPORATION 1720 Randolph Road, S.E. Albuquerque, New Mexico 87106		10. PROGRAM ELEMENT, PROJECT, TASK AREA & WORK UNIT NUMBERS
11. CONTROLLING OFFICE NAME AND ADDRESS OFFICE OF NAVAL RESEARCH 800 North Quincy Street Arlington, Virginia 22217		12. REPORT DATE September 1982 13. NUMBER OF PAGES 21
14. MONITORING AGENCY NAME & ADDRESS (if different from Controlling Office)		15. SECURITY CLASS. (of this report) UNCLASSIFIED 15a. DECLASSIFICATION DOWNGRADING SCHEDULE

16. DISTRIBUTION STATEMENT (of this Report)

Approved for Public Release - Distribution Unlimited

17. DISTRIBUTION STATEMENT (of the abstract entered in Block 20, if different from Report)

18. SUPPLEMENTARY NOTES

Earlier reports in this series are AMRC-R-332, AMRC-R-354, and AMRC-N-207.

19. KEY WORDS (Continue on reverse side if necessary and identify by block number)

Racetrack Electron Accelerator
Beam Breakup Instability
Image Displacement Instability

20. ABSTRACT (Continue on reverse side if necessary and identify by block number)

Beam breakup and image displacement instability growth rates for a 1 kA, 40 MeV electron beam racetrack induction accelerator are computed. The hypothetical device is taken to have four acceleration gaps, each with 0.2 MeV applied voltage and 15 ohm transverse impedance; the guide field is 2 kg. We find that the total amplification of the beam breakup mode is limited to 3.6 provided the cavity mode quality factor Q is 6. Image displacement mode growth is negligible. Thus, the negative mass instability, which grows about three

DD FORM 1 JAN 73 1473 EDITION OF 1 NOV 65 IS OBSOLETE

UNCLASSIFIED

SECURITY CLASSIFICATION OF THIS PAGE (When Data Entered)

times faster than the beam breakup instability for these parameters, is the dominant stability consideration. Probably, the negative mass instability can be controlled by sufficient spread in the electron energy.

CONTENTS

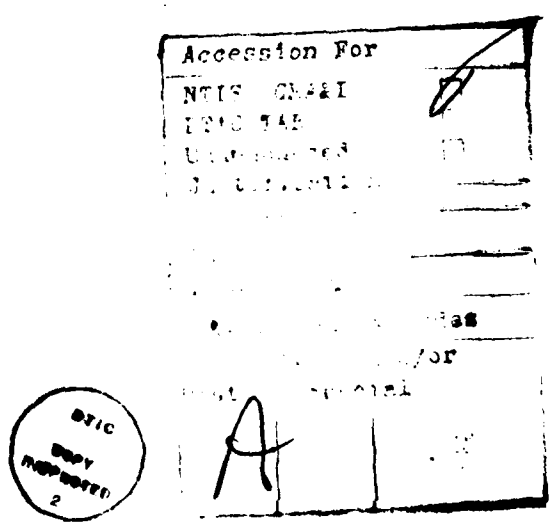

LIST OF ILLUSTRATIONS

LIST OF TABLES

I. INTRODUCTION

High current racetrack beam induction accelerators and modified betatrons are a subject of increasing interest as sources of high power electron beams for free electron lasers, flash radiography, and other applications. The racetrack induction accelerator geometry is illustrated in Figure 1. The beam is injected from a conventional pulsed diode beam generator into the drifttube, is progressively accelerated as it repetitively passes one or more induction modules, and then is extracted from the accelerator for its intended use. Beam extraction may even be unnecessary for microwave applications, because a slow-wave or rippled-magnetic-field cavity can be inserted in a straight section of the drifttube.[1]

Most beam stability studies for high current recirculating devices have dealt with negative mass and resistive wall instabilities.[2-5] However, experience with linear induction accelerators suggests that beam breakup and image displacement instabilities due to beam interaction with the induction modules and other discontinuities in the drifttube may be significant.[6,7] The beam breakup instability arises from a resonant coupling between beam transverse oscillations and m=1 electromagnetic cavity modes localized to the acceleration gaps,[8] while the image displacement instability is caused by interrupting the m=1 beam image current in the drifttube wall.[9] Clearly, the two are interrelated; in some contexts the image displacement instability can be viewed as the low frequency limit of the beam breakup instability.

This paper extends instability results developed for high current linear induction accelerators to cyclic devices. The primary differences are (1) that the beam passes the same few gaps again and again, and (2) that the curved beam trajectory couples longitudinal to transverse motion, perhaps leading to a hybridization of the negative mass and beam breakup modes. Experience with interaction among instabilities in other situations suggests that the latter item is the less important of the two.[10]

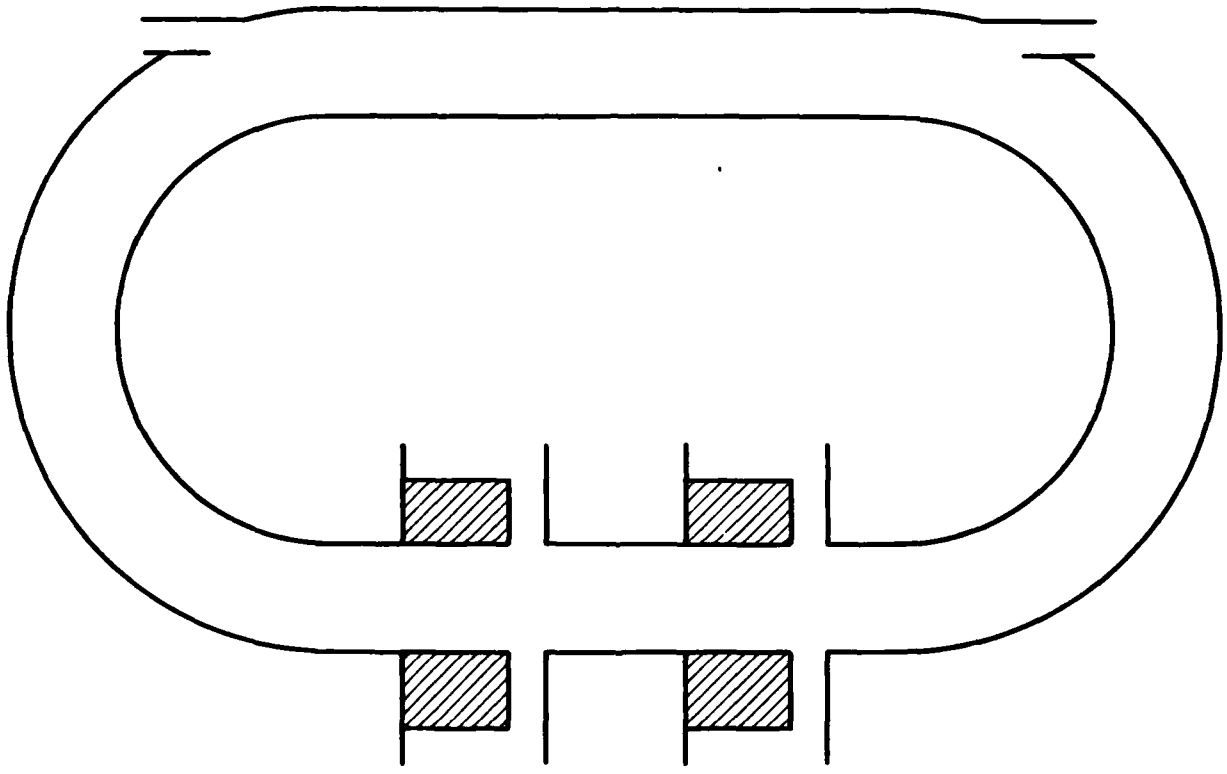

Figure 1. Simplified representation of cyclic induction accelerator with racetrack drift tube, acceleration gaps, and injection and extraction ports.

Therefore, we consider only the former aspect, periodicity of the interaction, and omit curvature effects. As in earlier calculations, we assume that the beam propagates at the speed of light, that lateral displacements of the beam are small and rigid, and that the gaps are narrow compared to the beam oscillation wavelength. The consequences of relaxing these approximations for the image displacement instability under different circumstances is discussed elsewhere.[9] We expect the three approximations to be adequate for present purposes.

A general dispersion relation for a multiple gap racetrack induction accelerator is derived in Section II. Because the resulting expression, a determinant, is cumbersome, we then specialize to the case of identical, uniformly spaced gaps, obtaining approximate analytical growth rate formulas for the beam breakup and image displacement instabilities. Section III illustrates instability growth for a 1 kA electron beam accelerated to 40 MeV through fifty cycles of a four gap device. (These parameters are based on an induction linac developed by the National Bureau of Standards and now being modified at the Naval Research Laboratory.[11]) First, growth rates are estimated based on the formulas of the preceding Section. Then, more precise numerical values are obtained with the beam transport code BALTIC, including the effects of acceleration and initial transients. Our findings, summarized in Section IV, are encouraging: The image displacement instability is negligible, and the beam breakup instability is manageable provided that the mode quality factor Q is kept low. A comparison with the negative mass and resistive wall instability growth rates also is provided.

II. DERIVATION OF GROWTH RATE EXPRESSIONS

In the long wavelength, paraxial approximation the linearized equation of transverse motion for the beam centroid is given by[9,10]

$$\left(\frac{d}{dt} + \frac{d}{dz}\right) \left[\gamma \left(\frac{d}{dt} + \frac{d}{dz}\right) - i\omega_c\right] \xi$$

$$- \frac{1}{2} \frac{\rho a^2}{\gamma^2 R^2} \xi = \sum F_j \delta(z - z_j) \xi \qquad (1)$$

Here, $\xi = x + iy$ is the (complex) transverse displacement of the beam centroid, ρ is the beam density, γ is the beam relativistic energy, a is the beam radius, R is the drifttube radius, and ω_c is the cyclotron frequency for the magnetic guide field. Time is normalized to the beam axial velocity, which is in turn assumed to be equal to the speed of light. The last term on the left side of Eq. (1) represents the combined transverse forces on the beam from its image charge and current in the smooth drifttube wall. Discontinuities in the wall are treated as impulsive forces appearing on the right side of Eq. (1).

We begin the derivation of the dispersion matrix by assuming the beam parameters to be constant in time and Fourier transforming Eq. (1).

$$\left(i\omega - \frac{d}{dz}\right) \left(i\omega - \frac{d}{dz} + i \frac{\omega_c}{\gamma}\right) \xi$$

$$- \frac{1}{2} \frac{\rho a^2}{\gamma^3 R^2} \xi = \frac{1}{\gamma} \sum F_j \delta(z - z_j) \xi \qquad (2)$$

As mentioned in the Introduction, we shall take account of time-varying γ in Sec. III by direct numerical integration of Eq. (1).

Next, Eq. (2) is solved for ξ, treating the right side of the equation as a source term. This can be done using a Green's function or, equivalently, by twice integrating the equation and imposing periodicity at z = L, the accelerator path length. The result is

$$\gamma(k_+ - k_-)\ \xi(z) =$$

$$(2\sin k_+ L/2)^{-1} \sum_{j=1}^{N} F_j\ \xi(z_j)\ \exp[ik_+(\mathrm{sign}[z_j - z]L/2 - (z_j - z))] \tag{3}$$

$$- (2\sin k_- L/2)^{-1} \sum_{j=1}^{N} F_j\ \xi(z_j)\ \exp[ik_-(\mathrm{sign}[z_j - z]L/2 - (z_j - z))]$$

where N is the number of acceleration gaps and Sign(x) is the sign of x. The wavenumbers $k_\pm$ characterize the beam cyclotron and spacecharge waves, respectively, as determined by the left side of Eq. (2), i.e., between gaps.

$$k_\pm = \omega + (\omega_c \pm [\omega_c{}^2 - 2\rho a^2/\gamma R^2]^{1/2})/2\gamma \tag{4}$$

For typical induction linac parameters, $k_+ \approx \omega + \omega_c/\gamma$ and $k_- \approx \omega$. Although it may not be immediately apparent, $\xi(z)$ as expressed in Eq. (3) is everywhere continuous; its first derivative is discontinuous at z_j.

Evaluating Eq. (3) at each of the gaps yields the system of equations

$$\gamma(k_+ - k_-)\ \xi\ (z_\ell) =$$

$$(2\sin k_+ L/2)^{-1} \sum_{j=1}^{N} F_j\ \xi(z_j)\ \exp[ik_+(L/2 - \mathrm{Mod}[z_j - z_\ell, L])] \tag{5}$$

$$- (2\sin k_- L/2)^{-1} \sum_{j=1}^{N} F_j\ \xi(z_j)\ \exp[ik_-(L/2 - \mathrm{Mod}[z_j - z_\ell, L])]$$

Here, Mod (x,L) is x modulo L, defined to lie between 0 and L. The determinant of the coefficient matrix of Eq. (5) is the desired dispersion relation. In general, it must be solved numerically to obtain ω. Additional analytical progress can, however, be made when the gaps are spaced uniformly and all have the same response function F.

$$\gamma(k_+ - k_-)\,\xi\,(\ell L/N) =$$

$$(2\sin k_+ L/2)^{-1}\ F \sum_{j=0}^{N-1} \xi(jL/N)\exp[ik_+(L/2 - \mathrm{Mod}[j-\ell,N]L/N)] \tag{6}$$

$$-\,(2\sin k_- L/2)^{-1}\ F \sum_{j=0}^{N-1} \xi(jL/N)\exp[ik_-(L/2 - \mathrm{Mod}[j-\ell,N]L/N)]$$

Since its right side is a discrete convolution, Eq. (6) is readily solved by performing a finite Fourier transform. We find

$$\gamma(k_+ - k_-) = iF\ \{\ (1 - \exp[2\pi im/N - ik_+ L/N])^{-1} - (1 - \exp[2\pi im/N - ik_- L/N])^{-1}\ \} \tag{7}$$

or, more simply,

$$1 = \frac{F}{2\gamma(k_+ - k_-)}\ \left\{\ \mathrm{ctn}\left[\frac{k_+ L/2 - \pi m}{N}\right] - \mathrm{ctn}\left[\frac{k_- L/2 - \pi m}{N}\right]\ \right\}. \tag{8}$$

The transform index m ranges between 0 and N-1. Still another useful representation, reminiscent of results for nonrecirculating devices, is[8,9]

$$\cos[(k_+ + k_-)L/2N - \pi m/N] =$$

$$\cos[(k_+ - k_-)L/2N] + \frac{F}{\gamma(k_+ - k_-)}\ \sin[(k_+ - k_-)L/2N]\ . \tag{9}$$

For F/ω_c small these equation are approximately satisfied by $k_+ \approx k_n$ or $k_- \approx k_n$, with $k_n \equiv 2\pi n/L$. Correspondingly,

$$\omega \approx \omega_n \equiv k_n - (\omega_c \pm [\omega_c^2 - 2\rho a^2/\gamma R^2]^{1/2})/2\gamma \ . \qquad (10)$$

Instability may occur when ω matches a resonant frequency of F or when the right side of Eq. (9) exceeds unity away from a resonance. These two possibilities are realized in the beam breakup and image displacement instabilities, respectively.

The beam breakup instability is caused by TM_{1n0} oscillatory electromagnetic fields localized to the acceleration gaps and adjacent drift-tube regions. These cavity modes are conveniently represented by damped harmonic oscillator equations for their normalized vector potentials.

$$\left(\frac{d^2}{dt^2} + \frac{\omega_o}{Q}\frac{d}{dt} + \omega_o^2\right) A_i = \frac{\omega_o Z_\perp}{2Q}\frac{\omega_o^2 \rho a^2}{2}\xi(z_i) \qquad (11)$$

Q is the cavity mode quality factor, while ω_o is its frequency. Coupling between the beam and a cavity mode is given by its transverse impedance $Z_\perp/Q$. The transverse impedance is basically a geometrical factor, which tends to scale linearly with the gap width.

Fourier transforming Eq. (11) in time, we obtain for $F = A/\xi$

$$F = -\frac{\omega_o^2}{\omega^2 + i\omega\omega_o/Q - \omega_o^2}\frac{\omega_o Z_\perp}{2Q}\frac{\rho a^2}{2} \ . \qquad (12)$$

The beam breakup instability growth rate now can be approximated in the usual manner by expanding Eq. (8) and (12) about ω_n, defined in Eq. (10). The resulting quadratic in $\omega - \omega_n$ shows instability only for $k_n \approx k_-$, with growth rate

$$\omega - \omega_n \approx i\frac{\omega_o}{2}\left\{\left[\frac{NZ_\perp}{2Q}\frac{\rho a^2}{\omega_c L} + \left(\frac{1}{2Q} - i\frac{\omega_n - \omega_o}{\omega_o}\right)^2\right]^{1/2} - \left(\frac{1}{2Q} - i\frac{\omega_n - \omega_o}{\omega_o}\right)\right\} \tag{13}$$

Note that this derivation fails for $\sin[(k_+ - k_-)L/2]$ too small; see Eq. (9). More precisely, the instability growth rate is reduced whenever $\left|Nk_n - \omega_c/\gamma\right|$ is less than the absolute value of the right side of Eq. (13) and finally vanishes when $Nk_n = \omega_c/\gamma$.

The image displacement instability arises due to interruption of the beam image current at a discontinuity in the drifttube wall, such as occurs at an acceleration gap. The analysis in Ref. 9 and 12 gives a force coefficient

$$F = \frac{\ell}{R^2}\frac{\rho a^2}{2} \tag{14}$$

The effective gap width ℓ is given by the physical width when the latter is small compared to the drifttube radius R. In the opposite limit, $\ell < R$. As already noted, growth occurs whenever the right side of Eq. (9) exceeds unity. For F/ω_c small this happens only in a narrow parameter region centered on $\tan[(k_+ - k_-)L/2] = F/\gamma(k_+ - k_-)$, for which the growth rate is

$$\Gamma \approx NF/\omega_c L. \qquad (15)$$

In the next section we evaluate these two growth rates for possible recirculating induction accelerator parameters and then generalize our numerical results to include irregular gap spacing and beam acceleration by computer solution of Eq. (1).

III. NUMERICAL EVALUATION OF GROWTH RATES

The four gap linear induction accelerator at the Naval Research Laboratory is an attractive candidate for a recirculating device. The acceleration gaps are in pairs with the members separated by about 30 cm. The distance between the two pairs is arbitrary within reasonable limits. Here we take the distance to be 200 cm, giving a total round-trip path length of L = 460 cm. (The specific value chosen does not strongly influence our conclusions.) The principle m=1 gap normal mode is at 880 MHz with a transverse impedance of 15 ohms and a Q of 60. Each gap provides an acceleration of 0.2 MeV, resulting in an energy gain for the electron beam of 40 MeV after 50 passes. A beam current of 1 kA and guide field of 2 kg are assumed. These parameters are summarized in Table 1. Note that γ in the table has been corrected for the spacecharge depression in the drifttube and also that $Z_\perp/Q$ has been expressed in dimensionless form by dividing the transverse impedance by 30 ohms.

Although the four gaps are not spaced uniformly, a reasonable upper bound on beam breakup instability growth can nonetheless be obtained from Eq. (13). We find $\Gamma = 12.9 \cdot 10^{-4}$ cm^{-1}, corresponding to about 30 e-foldings during the course of acceleration. (We assume $\omega_0 = \omega_n$.) The most obvious way of cutting this amplification to an acceptable level is by reducing Q. Recent work at Lawrence Livermore National Laboratory on short pulse induction accelerators suggests that a quality factor as low as

TABLE 1. NOMINAL RACETRACK INDUCTION ACCELERATOR PARAMETERS

Path Lengths	L = 460 cm	
Drifttube Radius	R = 7 cm	
Beam Radius	a = 1 cm	
Guide Field	B_z = 2 kg	(ω_c = 1.173 cm^{-1})
Beam Current	I = 1 kA	(ν = 0.0588)
Beam Energy	U = 0.4 - 40 MeV	(γ = 1.5 - 80)
Number of Gaps	N = 4	
Acceleration per Gap	ΔU = 0.2 MeV	($\Delta\gamma$ = 0.4)
Gap Resonant Frequency	880 MHz	
Mode Quality Factor	Q = 60	
Gap Transverse Impedance	15 ohms	($Z_\perp/Q$ = 0.5)
Gap Width	ℓ = 5 cm	

six is achievable.[13] For Q=6, $\Gamma = 2.4 \cdot 10^{-4}$ cm^{-1}, or 5.5 e-foldings. As many as eight e-foldings may be tolerable provided the gaps are not excited appreciably at their resonant frequency prior to beam injection.

More precise growth rates can be obtained by numerically solving Eq. (5) plus Eq. (12), and this is not difficult to do. Instead, we choose to integrate Eq. (1) plus Eq. (11) directly using the computer program BALTIC. The code was exercised extensively in support of the RADLAC radial pulseline accelerator program and so is well tested.[10] BALTIC has the advantage over a dispersion relation solver that it takes account of beam acceleration and of transients. It is, of course, much slower.

Table 2 summarizes thirteen runs of the BALTIC code. The quantities N, Q, ω_0, and γ were varied, but with $NZ_\perp/Q$ held fixed. Some calculations involved an accelerating beam. Cases 1-4 illustrate the effect of changing $\omega_0 - \omega_n$. Because $k_n = 0.014 \cdot n$ cm^{-1}, the pattern of growth rate variation with ω_0 in these four cases repeats itself with the same 0.014 cm^{-1} periodicity in ω_0. It so happens that $\sin[(k_+ - k_-)L/2]$ is small for $\gamma = 80$, the value chosen in cases 1-4, which reduces the growth rate some. Setting $\gamma = 60$ avoids this situation, increasing Γ by 25%, as illustrated in cases 5 and 6. The growth rate change caused by dropping Q from 60 to 10, as in case 7, is consistent with Eq. (13).

The seven cases just discussed were for a single gap. Cases 8 and 9 treat two gaps evenly spaced. Growth rates are comparable to the single gap runs, as expected. The enhancement of Γ for case 9 relative to case 8 again arises from adjusting $\sin[(k_+ - k_-)L/2]$.

Finally, cases 10-13 treat four gaps spaced as described at the beginning of this Section. Also, the beam is accelerating in these last four runs. It is clear from the resulting growth rates that the gradual acceleration which occurred has little effect on stability except to average

TABLE 2. SUMMARY OF BEAM BREAKUP INSTABILITY CALCULATIONS WITH BALTIC

Case	N	Q	ω_{o_1} (cm^{-1})	γ	Γ_4 (10^{-4} cm^{-1})
1	1	60	0.18	80	8.3
2	1	60	0.1732	80	3.3
3	1	60	0.17757	80	8.9
4	1	60	0.1787	80	8.8
5	1	60	0.18	60	10.0
6	1	60	0.17757	60	12.3
7	1	10	0.18	80	3.4
8	2	60	0.18	80	9.6
9	2	60	0.18	1.5	12.0
10	4	60	0.18	1.5-80	9.8
11	4	10	0.18	1.5-80	2.6
12	4	6	0.18	1.5-80	1.2
13	4	6	0.17757	1.5-80	1.6

over $\omega_0 - \omega_n$ and $\sin[(k_+ - k_-)L/2]$. In case 13, ω_0 was decreased slightly to maximize growth at large γ. Indeed, Γ increased by one-third relative to case 12.

Figure 2 depicts the maximum transverse displacement of the beam as a function of time for case 13. It and the other runs were initiated with a uniform transverse offset of unit magnitude for the beam. The cavity modes were initially excited at an amplitude consistent with injection of the offset beam with zero risetime, a worst case assumption. The displacement is seen to grow by a factor of about 3.6.

The image displacement instability turns out to be insignificant. From Eq. (15) its peak growth rate is $0.9 \cdot 10^{-4}$ cm^{-1}. Since this occurs only over a narrow range of parameters, however, we should expect a much slower average growth during acceleration. Indeed, a four gap BALTIC run gave no coherent growth whatsoever, and transient fluctuations amounted to less than 15% of the initial displacement.

IV. CONCLUSIONS

In this report we have developed a simple theory of beam breakup and image displacement instabilities in cyclic induction accelerators and applied it to obtain growth rate estimates for a possible device. The theoretical model takes recirculation into account primarily by enforcing periodicity on the unstable transverse models. Drifttube curvature effects were not considered. We find for the 1 kA, 40 MeV accelerator that neither the beam breakup nor the image displacement instability should be serious. Specifically, with Q=6 and parameters otherwise as in Table 1 the beam breakup growth rate is $\Gamma \approx 1.6 \cdot 10^{-4}$ cm^{-1}; the image displacement growth is negligible.

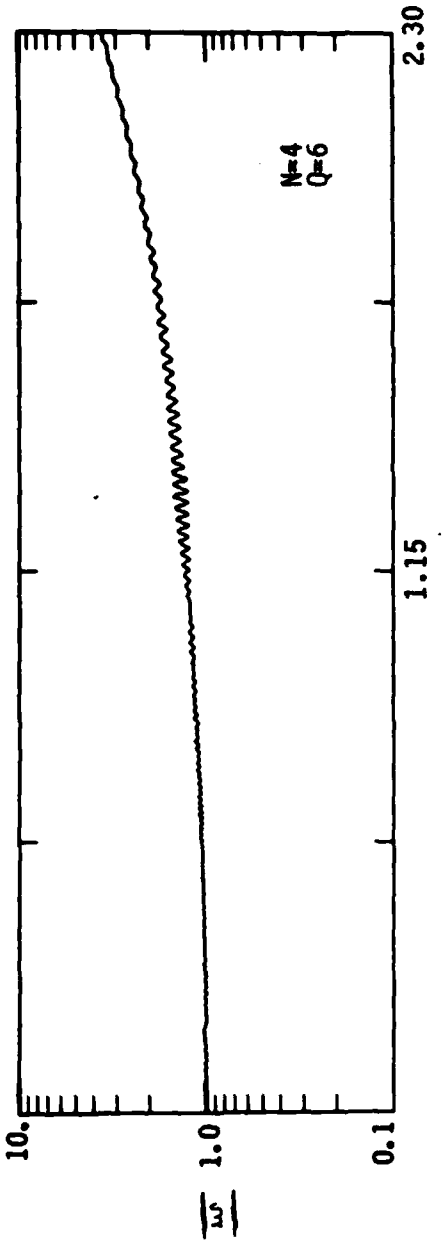

Figure 2. Time history of maximum beam transverse displacement for case 13 of Table 2.

For comparison, growth rates of the negative mass and resistive wall (for stainless steel) instabilities for comparable parameters are of order $5 \cdot 10^{-4}$ cm^{-1} and $0.2 \cdot 10^{-4}$ cm^{-1}, respectively.[3-5] Thus, the negative mass instability is somewhat more serious than the gap-induced instabilities in this instance.

The accelerator path length L = 460 cm chosen for the numerical calculations is perhaps small for practical devices. Increasing L by lengthening the straight sections of the racetrack geometry would have little impact on any but the resistive wall instability integrated growth: Growth rates of the gap-induced instabilities decrease roughly as L^{-1}, so that growth per pass remains fixed, while the negative mass instability grows only in the curved sections of the drift tube. In fact, the negative mass mode may decay in straight sections. Growth per cycle of the resistive wall instability, of course, increases linearly with L. Its growth rate is so slow, however, that the path length could be increased by an order of magnitude or more before the resistive wall instability became competitive with the other modes.

The important stabilizing influences of electron energy spread and transverse oscillations have been omitted from our calculations. Recent estimates for betatrons with comparable parameters suggest that a 10% spread in the injected beam electron energies is sufficient to suppress the negative mass instability provided that the mean injection energy is greater than about 3 MeV.[2-5] Additionally, research in support of the ATA accelerator program predicts that employing occasional nonlinear focusing elements to spread the electron transverse oscillation frequencies can limit beam breakup instability growth.[14] We remark also that varying the resonant frequencies ω_0 from gap to gap can cut the beam breakup growth rate by N^{-1}, provided the relative shifts are greater than Q^{-1}.[15]

Extensions to the present research naturally fall into two categories, adding drifttube curvature and adding beam temperature. The former is relatively easily accomplished by inserting the transport equations of Ref. 4 or 16 into BALTIC. This also would allow us to determine the influence of straight drifttube sections on the negative mass instability. Treating beam temperature beyond what has already been done probably requires numerical simulation.

REFERENCES

1. C. W. Roberson, "The Racetrack Induction Accelerator," IEEE Nuc. Sci. NS-28, 3433 (1981).

2. P. Sprangle and J. L. Vomvoridis, "Longitudinal and Transverse Instabilities in a High Current Modified Betatron Electron Accelerator," NRL-4688 (Naval Research Laboratory, Washington, 1981).

3. B. B. Godfrey and T. P. Hughes, "Resistive Wall Instabilities in the Modified Betatron," AMRC-R-332 (Mission Research Corporation, Albuquerque, 1981).

4. T. P. Hughes and B. B. Godfrey, "Linear Stability of the Modified Betatron," AMRC-R-354 (Mission Research Corporation, Albuquerque, 1982).

5. B. B. Godfrey and T. P. Hughes, "Modified Betatron Stability Calculations," AMRC-N-207 (Mission Research Corporation, Albuquerque, 1982).

6. T. J. Fessenden, W. A. Atchison, D. L. Birx, R. J. Briggs, J. C. Clark, R. E. Hester, V. K. Neil, A. C. Paul, D. Rogers, and K. W. Struve, "Physics of a Repetitively Pulsed 10 kAmp Electron Beam," Proc. 4th Conf. Electron and Ion Beam Research and Technology (Palaiseu, 1981), p. 813.

7. R. B. Miller, J. W. Poukey, B. G. Epstein, S. L. Shope, T. C. Genoni, M. Franz, B. B. Godfrey, R. J. Adler, and A. Mondelli, "Beam Transport in High Current Linear Accelerators," IEEE Nuc. Sci. NS-28, 3343 (1981).

8. V. K. Neil, L. S. Hall, and R. K. Cooper, "Further Theoretical Studies of the Beam Breakup Instability," Part. Accel. 9, 213 (1979).

9. R. J. Adler, B. B. Godfrey, M. M. Campbell, and D. J. Sullivan, "The Image Displacement Effect in Intense Electron Beams," AMRC-R-333 (Mission Research Corporation, Albuquerque, 1982).

10. R. J. Adler and B. B. Godfrey, "Study of High Current Induction Linac Phenomena: Experiment and Theory," AMRC-R-411 (Mission Research Corporation, Albuquerque, 1982); and references therein.

11. J. E. Leiss, N. J. Norris, and M. A. Wilson, "The Design and Performance of a Long-Pulse High-Current Linear Induction Accelerator at the National Bureau of Standards," Part. Accel. 10, 223 (1980).

12. V. K. Neil, "The Image Displacement Effect in Linear Induction Accelerators," UCID-17976 (Lawrence Livermore National Laboratory, Livermore, 1978).

REFERENCES (Continued)

13. D. L. Birx, "Reduction of the Beam Breakup Mode Q Values in the ETA/ATA Accelerating Cells," UCID-18630 (Lawrence Livermore National Laboratory, Livermore, 1980).

14. E. P. Lee and others, private communication.

15. B. B. Godfrey and R. J. Adler, unpublished.

16. D. P. Chernin and P. Sprangle, "Transverse Beam Dynamics in the Modified Betatron," NRL-4687 (Naval Research Laboratory, Washington, 1981).